MODELLING THE STRUCTURAL RESPONSE OF FIBRE-REINFORCED COMPOSITES SUBJECTED TO FIRE

R. Gutkin[a*], H. Olsen[b], P. Blomqvist[b]

[a]*Swerea SICOMP AB, SE-431 22, Mölndal, Sweden.*
[b]*SP Fire Research, SP Technical Research Institute of Sweden, PO Box 857, S-501 15 Borås, Sweden.*
**renaud.gutkin@swerea.se*

Keywords: fire, degradation, failure

Abstract

The present contribution details the development and implementation of dedicated material models for the finite element computation of the thermal and mechanical response of polymer composite structures subjected to fire. The material models are developed so that mechanical and thermal properties at the ply level can be calculated from the constituent's properties, therefore allowing for a greater flexibility in architecture and reduced testing programs.
The degradation of the resin during fire is predicted during the thermal analysis. Its effect, together with the effect of temperature, on the mechanical response is accounted for in the material model. The models are validated against a mini furnace experiment.

1. Introduction

Fire is a common and critical threat to fibre-reinforced polymer composite structures. Unlike metals, the organic resin used to produce composites is reactive at high temperature and decomposes when exposed to fire. Understanding and being able to model the fire structural performance is a critical safety issue as the decomposing resin will result in loss of stiffness and strength, leading to distortion and possible collapse of the structure.
Computational modelling of the fire-structural response is a multi-physics problem which can be divided into four steps: modelling of (i) the fire environment, (ii) thermal response of materials, (iii) fire-induced damage and weakening of materials, and (iv) the mechanical response of the structure. Advanced fire-structural modelling requires either integration of these models into a single piece of software or coupling of software developed for the specific tasks.

The fire environment can be computed using the Computation Fluid Dynamics (CFD) software Fire Dynamics Simulator (FDS). The results in terms of heat flux and temperature are then transferred and interpolated to the structural Finite Element (FE) model in ABAQUS, using for example the interoperability tool developed in [1].
The present work focuses on the FE analyses, which consist of a heat transfer analysis followed by a mechanical analysis. Ramroth [2] followed such a strategy and developed both a thermal and a material model for the analysis of composite sandwich panels exposed to fire. The thermal model accounts for the heat transfer, the thermal decomposition of the resin, and the resulting mass transfer. The material model developed is elastic-viscoplastic. Zhang [3] followed a similar approach and developed a three-dimensional model including the effect of

orthotropic viscoelasticity and resin decomposition. The focus is on monolithic composites and only a failure criterion for compressive failure is implemented.
The thermal model presented in this report is similar to the one in [2] and originates from the model presented in [4]. The material model is simplified to piecewise linear elasticity.

2. Experimental work

A lightly loaded sample of the commingled material COMFIL-G has been tested on a vertical mini furnace. A 300x300x10 mm sample was exposed to standard fire testing time temperature conditions. The load was applied with a steel weight of 12.8 kg on a steel strip, as shown in Figure 1, and the load displacement was measured with linear transducers. Temperatures were recorded at 9 mm and on the unheated surface.

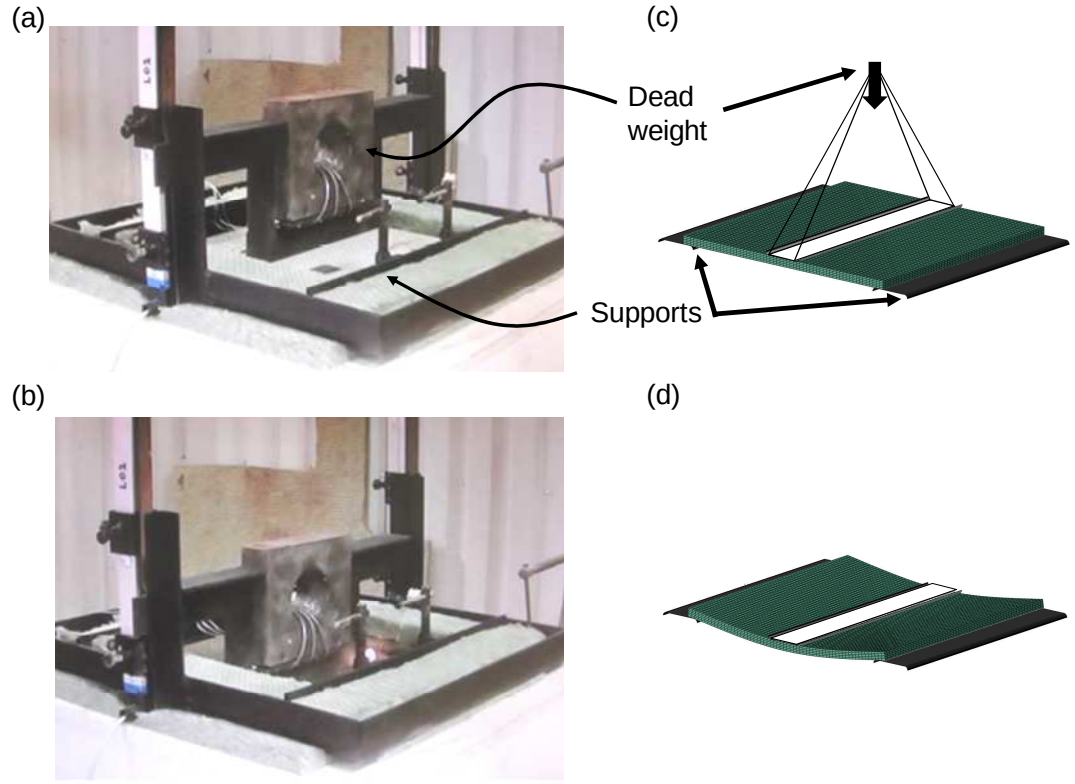

Figure 1 (a) and (b) Loaded plate in mini furnace before and after testing. (c) and (d) Finite element model in underformed and at maximum deflection.

3. Numerical model

3.1. Thermal model

The model developed here is based on a model proposed by Henderson [4], in which the energy conservation for one dimensional heat transfer in a polymer composite undergoing thermal decomposition is written as

$$\rho C_p \frac{\partial T}{\partial t} = k \frac{\partial^2 T}{\partial x^2} + \frac{\partial k}{\partial x}\frac{\partial T}{\partial x} - \dot{m}_g C_{pg} \frac{\partial T}{\partial x} - \frac{\partial \rho}{\partial t}\left(Q_i + h - h_g\right) \quad (1)$$

$$\frac{\partial \rho^r}{\partial t} = -Ae^{-\frac{E}{RT}}\rho_0 \left(\frac{\rho^r - \rho^r{}_f}{\rho^r{}_0}\right)^n \tag{2}$$

Equation (1) is solved using the Finite Element (FE) method. The last term in Equation (1) is calculated using a user defined subroutine (HETVAL) which provides internal heat generation. The ordinary differential equation in $\partial \rho^r \,/\, \partial t$ defined by the Arrhenius above is solved using a fourth order Runge-Kutta method.

The residual resin content is introduced as

$$F = \frac{\rho^r - \rho^r_{ch}}{\rho^r_v - \rho^r_{ch}} \tag{3}$$

where ρ^r is the density of the resin and the subscript *v* and *ch* refers to the virgin and char material, respectively. The thermal conductivity of the resin is expressed as

$$k^r = Fk^r_v + (1-F)k^r_{ch} \tag{4}$$

and the longitudinal and transverse conductivities of the composites are calculated as

$$k_{11} = v_f k^f + \left(1 - v_f\right)k^r \tag{5}$$

$$k_{22} = k_{33} = k^r \left(\frac{1 + \xi^{thermal}\eta^{thermal}v_f}{1 - \eta^{thermal}v_f}\right) \tag{6}$$

where v_f and k^f are the fibre volume fraction and the conductivity of the fibres, respectively. Finally, we calculate the specific heat capacity of the resin as a function of the variable *F*.

$$C^r_p = FC^r_{pv} + (1-F)C^r_{pch} \tag{7}$$

and the specific heat capacity of the composite as

$$C_p = \left(v_f \rho^f C^f_p + \left(1 - v_f\right)\rho^r C^r_p\right)/\rho \tag{8}$$

where C^f_p is the specific heat capacity of the fibres.

3.2. Material model

The material is assumed to be linear elastic and the elastic constants are all assumed to be temperature and resin residual content dependent, except for the Poisson's coefficients. The dependencies are expressed as in [5] and as shown in Equation (9). The properties required in Equation (9) are measured for the resin (E^{m} and X^{m}), then the undamaged (U) and residual (R) properties are calculated for the ply properties using the micromechanical relationships detailed in Equation (10) to (16) [6].

$$P(T) = \left(\frac{P_U + P_R}{2} - \frac{P_U - P_R}{2}\tanh\left(k(T - T')\right)\right)F^n \tag{9}$$

$$E_{11} = v_f E^f + \left(1 - v_f\right)E^m \tag{10}$$

$$E_{22} = E_{33} = E^m\left(\frac{1 + \xi_E^{mech}\eta_E^{mech}v_f}{1 - \eta_E^{mech}v_f}\right) \tag{11}$$

$$G_{23} = \frac{E_{22}}{2(1 + \nu_{23})} \tag{12}$$

$$G_{12} = G_{13} = G^m\left(\frac{1 + \xi_G^{mech}\eta_G^{mech}v_f}{1 - \eta_G^{mech}v_f}\right) \tag{13}$$

with

$$\xi_E^{mech} = \xi_G^{mech} = 2 \tag{14}$$

$$\eta_E^{mech} = \left(\frac{(E^f/E^m) - 1}{(E^f/E^m) + \xi_E^{mech}}\right) \tag{15}$$

$$\eta_G^{mech} = \left(\frac{(G^f/G^m) - 1}{(G^f/G^m) + \xi_G^{mech}}\right) \tag{16}$$

Figure 2 and Figure 3 show the variation in elastic properties for the resin (PA-6) alone and the unidirectional COMFIL material using Equation (11) to (17). The thermal properties and mechanical properties are given in Table 1 and Table 2.

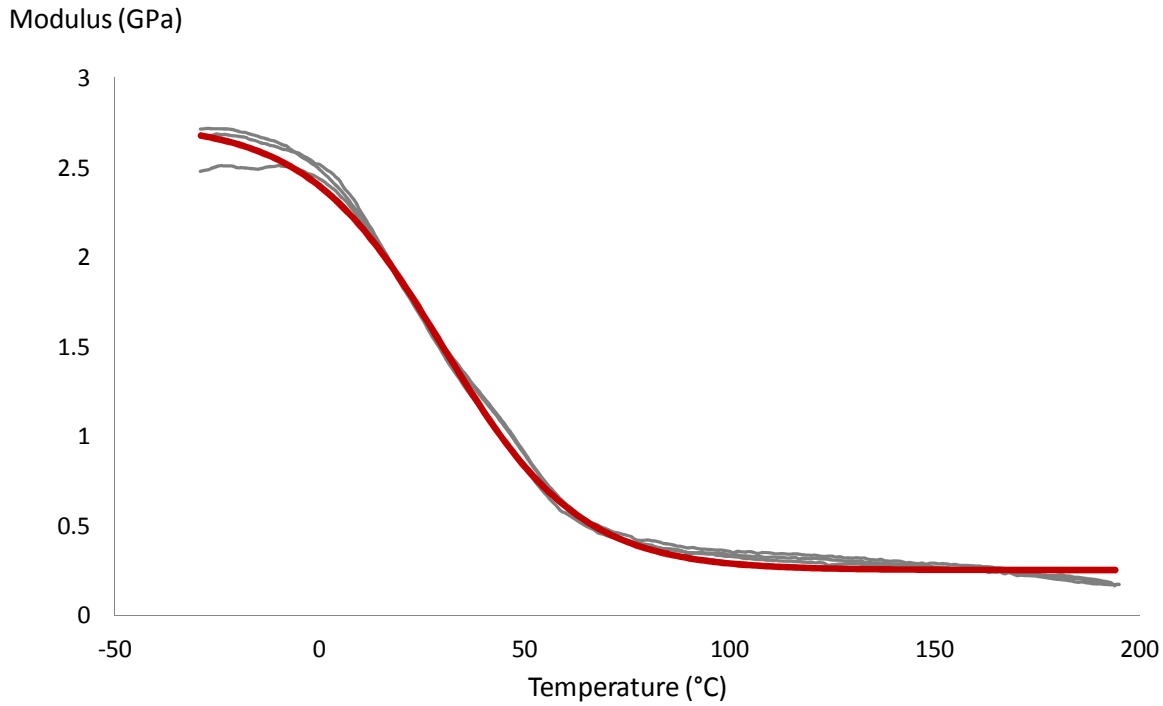

Figure 2 Young's modulus of the resin as a function of the temperature.

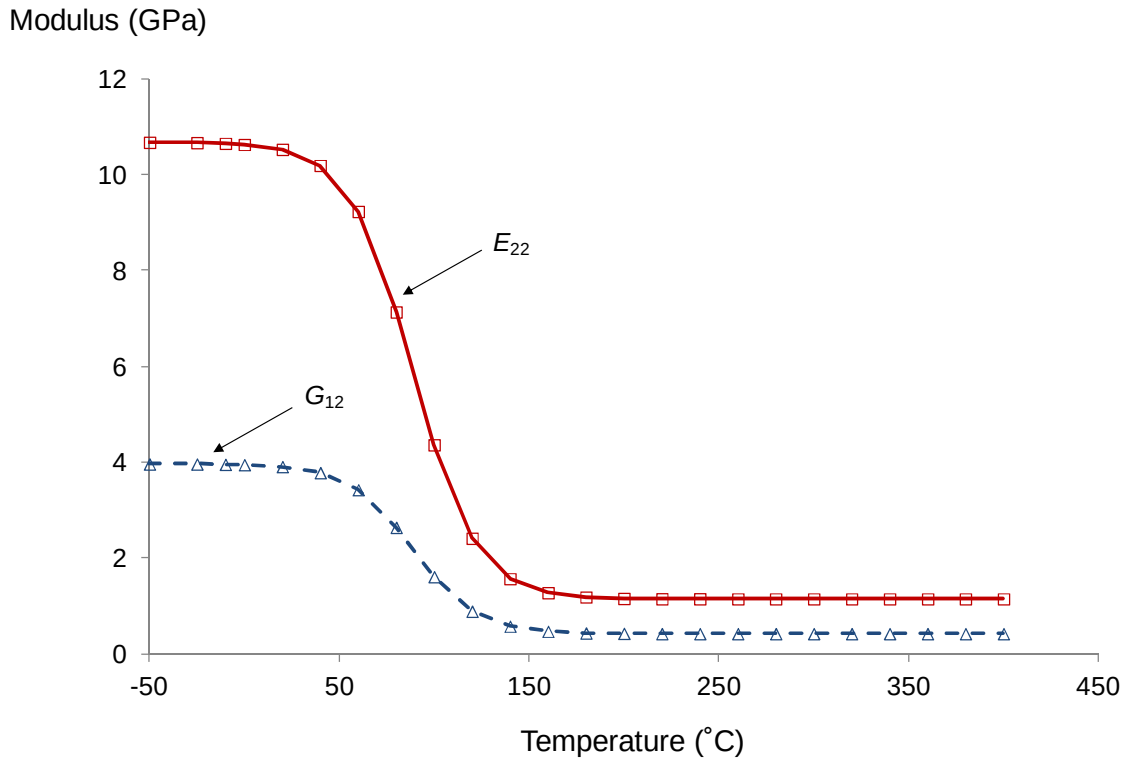

Figure 3 Shear and transverse moduli of the composite as a function of the temperature.

v_f	A	E
( )	**(1/s)**	**(J/(kg mol))**
0.51	2.59E11	186 400

Final remaining resin content (%)	**Heat of decomposition (J/kg)**	**Specific heat glass (J/(kg K))**
3	378,800	0.3
Specific heat (J/(kg K))	**Thermal conductivity (W/(m K))**	**Density (kg/m^3)**
1060+1.4xT(˚C)	0.6	1908

Table 1. Thermal properties.

E_U^m **(GPa)**	E_R^m **(GPa)**	k	T' **(˚C)**	ν **( )**
2.75	0.025	0.03	30	0.36

Table 2. Mechanical properties of the resin.

3.3. Finite element model

For the thermal part, a three dimensional FE model of the mini furnace is created using DC3D8 quadrilateral elements. On the hot face, a temperature load is directly applied and such that the temperature at one millimeter from the hot face matches the measured temperature profile. On the cold face both radiative and convective boundary conditions are applied where an emissivity of 0.9 is used for the radiative part, and for the convective part, a coefficient of convection of 15 W m^{-2} K^{-1} and a temperature of 23˚C is chosen for the sink temperature. For the mechanical part, the finite element model is the same as the thermal model, with the exception that thermal elements are replaced by C3D8R solid elements. The weight and supports are modeled as rigid body and a frictionless contact is defined between these parts and the plate.

4. Results

4.1. Temperature profile

Both the numerical and experimental temperature profiles at the cold and hot faces are shown in Figure 4. The experimental profiles show a discontinuity at approximately 360 s which correspond to the time at which the plate falls into the mini furnace. The highest temperature reached into the plate is approximately 250℃ which implies that no pyrolysis takes place, as the threshold temperature for this is 380℃.

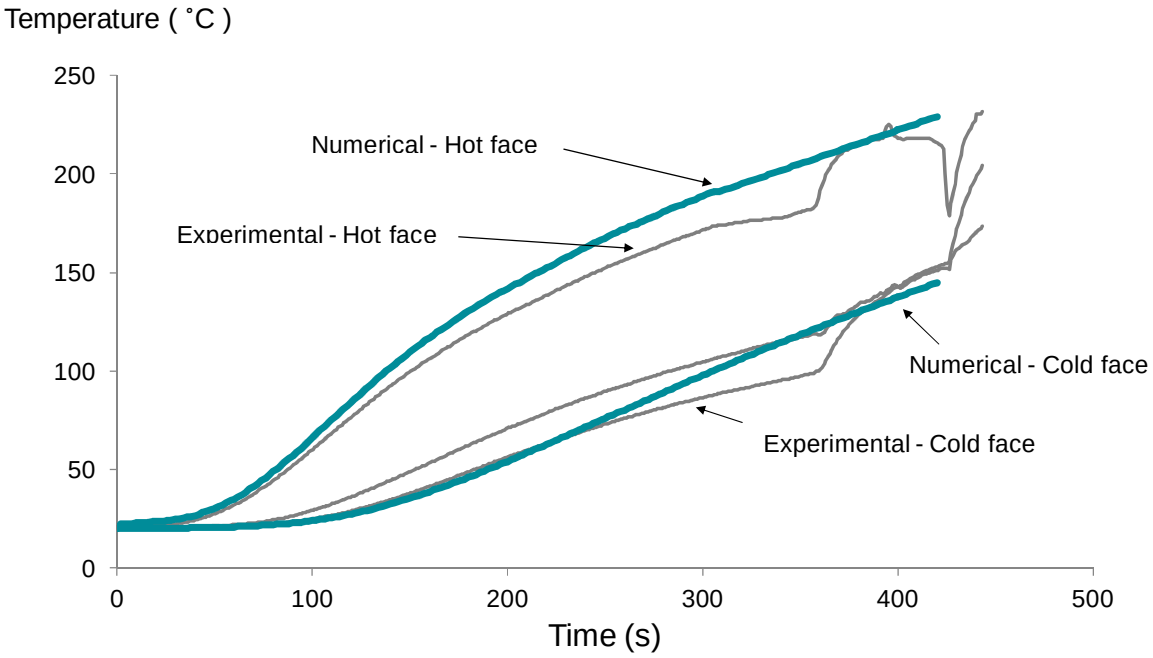

Figure 4 Numerical and experimental temperature profile on the hot and cold faces.

4.2. Deflection

Figure 5 show the experimental and numerical deflection of the plate during testing. The test specimens fails and collapses into the furnace after six minutes test time, when the unexposed surface temperatures are at 100˚C. Failure is also clearly visible from the readings of the linear transducers where a step change is noted at six minutes.

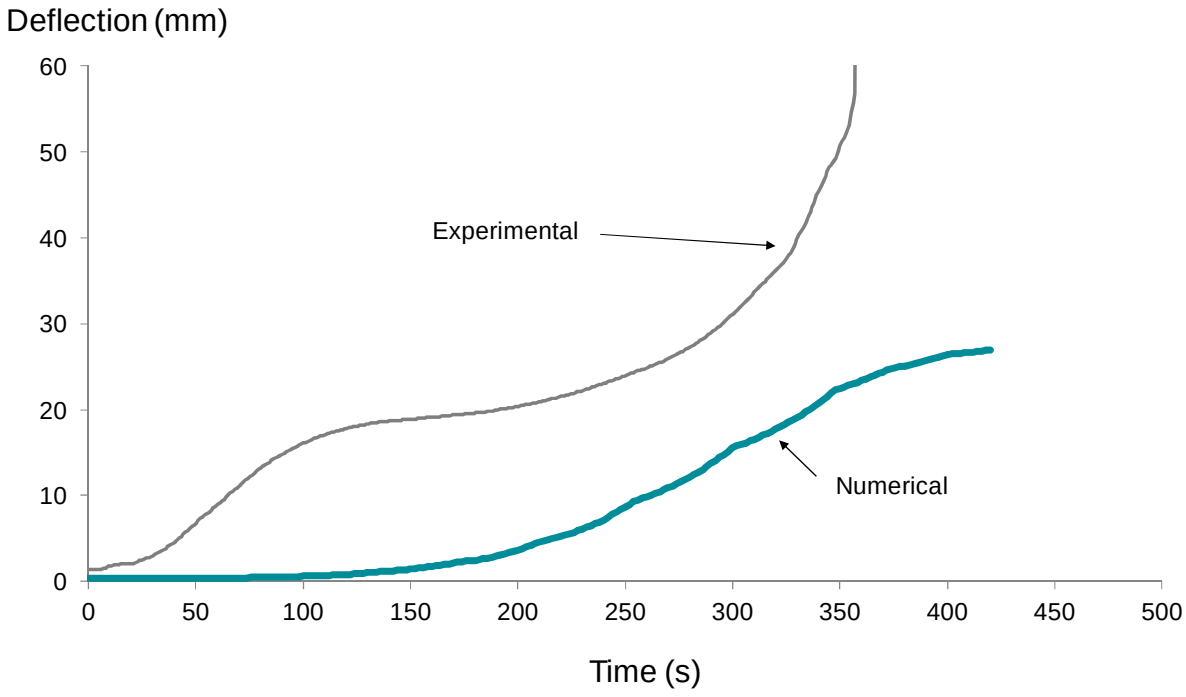

Figure 5 Experimental and numerical deflection of the plate during the test.

5. Discussion

The temperature profiles predicted by the model are in good agreement with the experiments. This indicates that the material model during the thermal analysis performs well. It should however be noted that no degradation of the resin is obtained during the test and therefore the performance of the model in that respect is not validated.
The deflection predicted by the model is lower that the deflection measured experimentally. In particular, the increase in deflection at 100 s is not predicted. This is believed to come from the creep behaviour of the resin which is not accounted for in the model. The final collapse of the specimen observed experimentally corresponds to the fall of the plate in the furnace. This event is not expected to be captured numerically as the implicit solver used here does not allow for rigid body motion.

6. Conclusions

A simulation chain to predict both thermal and mechanical responses of a composite structure subjected to fire has been presented. The thermal part is well predicted while improvements are needed for the mechanical part. In particular, the creep behaviour of the composite needs to be accounted for.
The next element to be added in the chain is the simulation of the fire dynamics which will provide more exact and realistic boundary conditions to the thermal analysis.

7. Acknowledgements

Majority of this work has been carried out within the EU-project FIRE-RESIST.
Spyros Tsampas is gratefully acknowledged for the DMTA tests performed on the PA-6 resin.

References

[1] A. Paajanen, T. Korhonen, M. Sippola, S. Hostikka, M. Malendowski, R. Gutkin. FDS2FEM – a tool for coupling fire and structural analyses. In *Proceedings of IABSE Workshop Helsinki 2013 Safety, Failures and Robustness of Large Structures*, Helsinki 2013.

[2] W. T. Ramroth. Thermo-mechanical structural modelling of FRP composite sandwich panels exposed to fire. *PhD thesis University of California*, 2006.

[3] Z. Zhang Z. Thermo-Mechanical Behavior of Polymer Composites Exposed to Fire. *PhD thesis Virginia Polytechnic Institute and State University*, 2010.

[4] J.B. Henderson, T.E. Wiecek (1987). A Mathematical Model to Predict the Thermal Response of Decomposing, Expanding Polymer Composites. *Journal of Composite Materials*, 21, 373 – 393, 1987.

[5] A.G. Gibson, T.N.A. Browne, S. Feih, A.P. Mouritz. Modelling high temperature behaviour and fire response under load. *Journal of composite materials*, 46, 2005 – 2022, 2012.

[6] J.C. Halpin, S.W. Tsai. Effects of environmental factors on composite materials, *AFML-TR 67 - 423, Dayton OH*, 1969.